# A Comprehensive Review on Research Methods for Lithium-ion Battery of State of Health Estimation and End of Life Prediction: Methods, Properties, and Prospects

Jiahui Ren, Jinkai Ma, Honghong Wang, Teng Yu, and Kai Wang

***Abstract*—Recently, lithium-ion batteries (LIBs) have become the leading energy storage solution for electric vehicles due to their high energy density and long lifespan. Examining the health condition of LIBs is essential for their safe and reliable operation. This paper thoroughly assesses the latest researches on techniques for forecasting the health of LIBs, examines the properties of diverse methodologies, and proposes future development directions. First, the aging mechanism of lithium-ion batteries is introduced and the factors affecting battery aging are explored. Then, based on different prediction objectives, the prediction of lithium-ion battery health is divided into state of health (SOH) estimation and end of life (EOL) prediction. The SOH estimation methods are introduced from model-based and data-driven methodologies, while the EOL prediction is focused on the data-driven methods. Finally, the future development direction of LIB health prediction is identified, and four new potential topics on battery prediction are proposed.**

***Index Terms*—Lithium-ion batteries, state of health, end of life, estimation methods.**

## NOMENCLATURE

### *A. Abbreviations*

| | |
|---|---|
| CNN | convolutional neural network |
| DT | decision tree |
| DepSep conv | depthwise separable convolution |
| ECM | equivalent circuit model |
| EIS | electrochemical impedance spectroscopy |
| EKF | extended Kalman filter |
| EKPF | extended Kalman particle filter |
| EM | electrochemical model |
| EMD | empirical mode decomposition |
| EOL | end of life |
| ESR | equivalent series resistance |
| FOM | fractional order form |
| GBDT | gradient boosting decision tree |
| GPR | Gaussian process regression |
| GRU | gated recursive unit |
| IOM | integer order mode |
| IR | increase of internal resistance increase |
| KF | Kalman filter |
| LAM | loss of active material |
| LIB | lithium-ion battery |
| LKF | linear Kalman filter |
| LLI | loss of lithium inventory |
| LSTM | long-term short-term memory neural networks |
| NLKF | nonlinear Kalman filter |
| PCC | Pearson correlation coefficient |
| PF | particle filter |
| PNGV | partnership for a new generation of vehicles |
| PRBM | polynomial regression based battery model |
| P2D | pseudo two-dimensional |
| RF | random forest |
| RLS | recursive least squares |
| RMSE | root mean square error |
| RNN | recurrent neural network |
| SEI | solid electrolyte interface |
| SOC | state of charge |
| SOH | state of health |
| SP | single particle |
| SPM | single particle model |
| VMD | variational mode decomposition |

### *B. Variables*

| | |
|---|---|
| $\boldsymbol{Q}$ | covariance matrix |
| $C_{\text{aged}}$ | current capacity |
| $C_{\text{rated}}$ | rated capacity |

Received: June 1, 2024
Accepted: September 1, 2024
Published Online: May 1, 2025

Jiahui Ren, Jinkai Ma, Honghong Wang, and Kai Wang (corresponding author) are with the School of Electrical Engineering, Qingdao University, Qingdao 266000, China (e-mail: renjiahui6608@gmail.com; QDUmjk@163.com; sdwhh2007@126.com; wkwj888@163.com).

Teng Yu (corresponding author) is with the School of Electronic and Information Engineering, Qingdao University, Qingdao 266000, China (e-mail: yutenghit@foxmail.com).

DOI: 10.23919/PCMP.2024.000211

| | |
|---|---|
| $f$ | activation function |
| $H$ | number of leaf nodes |
| $\boldsymbol{K}_k$ | Kalman gain matrix |
| $\boldsymbol{P}_0$ | error covariance |
| $Q_{\text{aged(max)}}$ | current maximum battery discharge capacity |
| $Q_{\text{new(max)}}$ | maximum discharge capacity of new battery |
| $R_{\text{BOL}}$ | new battery internal resistance |
| $R_{ct}$ | charge transfer resistance |
| $R_{\text{EOL}}$ | internal resistance at EOL |
| $R_{\text{NOW}}$ | internal resistance of the current battery |
| $R_{\text{SEI}}$ | solid-electrolyte interphase resistance |
| $s_k$ | measurement noise |
| $V_{\text{RC,s,k}}$ | slow component of transient voltage |
| $W_{ij}$ | weight between the input and the *j*th output |
| $x_i$ | *i*th input |
| $\overline{x_0}$ | average value of the initial state |
| $y_j$ | *j*th output of the neuron |
| $y_k$ | system measurements |
| $\overline{y_k}$ | system output |
| $\beta_i$ | true value |
| $\overline{\beta_i}$ | predicted value |
| $\eta$ | leaf weight values |
| $\varphi$ | a leaf weight penalty factor |
| $\delta$ | iteration of the objective function |

## I. Introduction

The use of nonrenewable resources such as oil, coal, and natural gas has caused irreversible climate phenomena on earth, and thus, there is urgent need to use science and technology to find alternative energy sources [1]. Lithium-ion batteries (LIBs) offer several advantages, including high energy density, minimal self-discharge, absence of memory effect, and long lifespan, thus making them the preferred choice for electrochemical energy storage systems. Currently, they are extensively utilized in electric vehicles, electric ships, and electric aircraft [2]–[5]. In addition, LIBs are widely employed in the fields of satellites, laptop computers, and smart power grids [6]. LIBs offer high profitability, attracting significant investment to enhance their stability and recyclability. Despite their high initial costs, LIBs continue to command a substantial market presence [7]. However, LIBs encounter numerous challenges, while the prediction of LIBs capacity degradation is beneficial for the optimization of interdisciplinary energy operation and the improvement of energy system efficiency and reliability [8], [9].

This paper examines and assesses the aging process of LIBs and the factors that impact their aging. This study also outlines predictive methods for monitoring battery health and identifies key challenges and outlooks in current battery health monitoring research. The advancement can help to foster the progress of new energy batteries and enhance the global new energy landscape. Compared with previous reviews, the main highlights of this paper include:

1) Review the aging mechanism and influencing factors of LIBs.

2) Divide battery health prediction methods into model-based and data-driven approaches, and evaluate various prediction methods.

3) Provide new research directions for future lithium-ion health estimation methods, and propose recommendations and prospects for advancement.

4) Summarize many advanced research achievements in the past three years.

The organization of this paper is described as follows. In Section II, the working principle and aging mechanism of LIBs are introduced, and their influencing factors are analyzed. In Section III, the sources of battery datasets are introduced, while the definition of the state of health (SOH) and its two major categories of monitoring methods are introduced in Section IV. Section V introduces the end of life (EOL) prediction based on data-driven methods, and various prediction methods are evaluated in Section VI. Finally, Section VII summarizes the future development direction and main challenges of LIBs.

## II. Working Principle and Aging Mechanism of Lithium-ion Batteries

Studying the working principle of LIBs can help to better understand the aging process of LIBs, and to use batteries correctly and delay the EOL of LIBs. The knowledge of the aging processes of LIBs will help draw the optimal strategies, increase the life cycle performance, and reach beyond the prescribed goals [8].

### *A. Working Principle of Lithium-ion Batteries*

The composition material of LIBs is mostly porous carbon, while graphite is generally used as the anode and metal oxide as the cathode [9], [10]. Typical anode materials consist of carbon-based compounds and lithium-containing alloys. Cathode materials are essential to the functioning of LIBs and must demonstrate exceptional electrochemical properties. A lithium salt containing lithium ions is present in organic carbonates that make up the electrolyte solution [11]. Similar to other battery technologies, the operational principle of LIBs can be summarized as the removal and insertion of lithium-ions [12]. As the discharge process unfolds, solid lithium is dispersed on the surface of the anode material for electrochemical reactions, causing lithi-

um-ions to transfer to the electrolytic solution [13]. The equilibrium equation for the reaction involving graphite as the cathode material is as follows:

$$\mathrm{Li}_x\mathrm{C}_6 \leftrightarrow \mathrm{LiC}_6 + x\mathrm{Li}^+ + x\mathrm{e}^- \quad (1)$$

Lithium ions disperse and conduct ions through the electrolyte sequentially, interact with the anode and return to solid status. In this case, the equilibrium reaction between the cathode and lithium metal oxide can be described as follows:

$$\mathrm{LiMO}_2 + y\mathrm{Li}^+ + y\mathrm{e}^- \leftrightarrow \mathrm{Li}_y\mathrm{MO}_2 \quad (2)$$

Lithium will remain stored in the battery until it is recharged later. During high current discharge, if the electrolyte surface becomes saturated or depleted, cells may suddenly lose power based on lithium concentration [14].

### *B. Aging of Lithium-ion Batteries*

Aging can be defined as a decrease in system performance, lifespan, and reliability, and battery aging may lead to capacity degradation, power degradation, or both. The electrochemical aging mechanism may differ among different types of LIBs [15]. Given the multitude of factors contributing to battery aging, investigating the aging mechanism of LIBs also presents certain challenges.

The calendar life of LIBs signifies the duration from the production date to the end of battery life. Calendar aging, or the aging produced during battery storage, is the non-reversible percentage of capacity loss during storage [16]. LIBs' cycle life, which is the upper limit of charging and discharging times, will decrease with battery aging. The aging mechanism principle of LIBs is shown in Fig. 1.

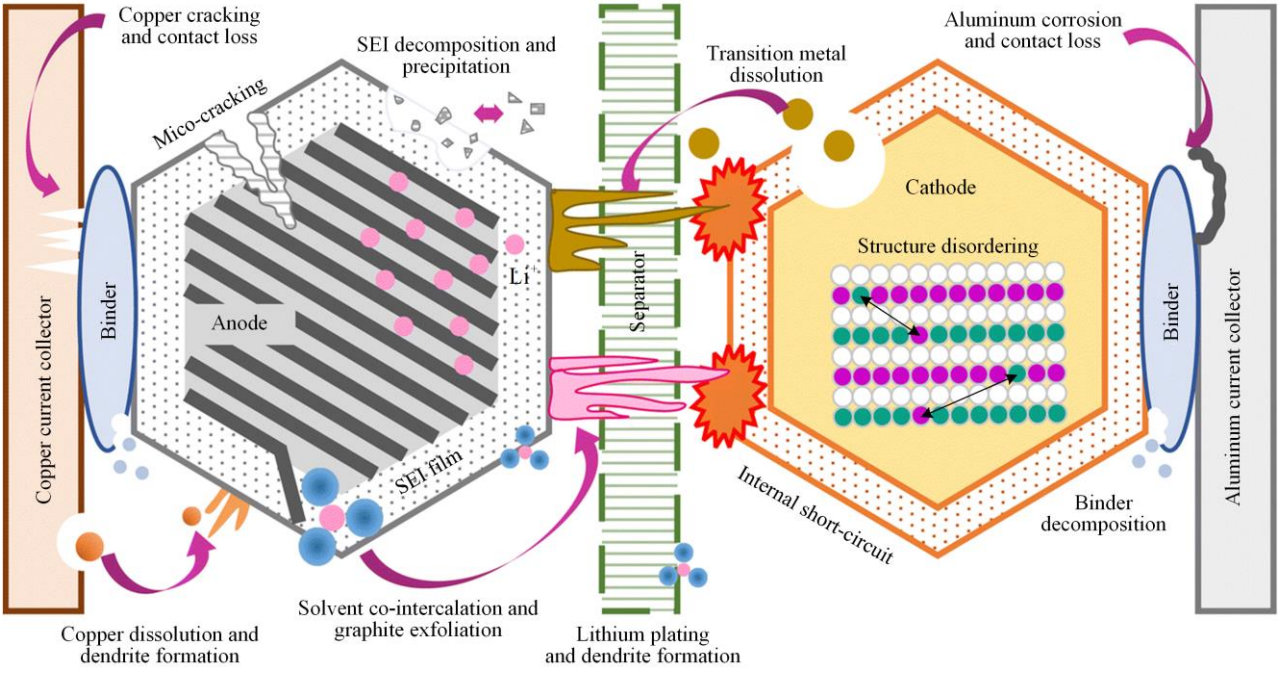


Fig. 1. Main aging mechanisms for lithium-ion batteries referring to [17] with permission.

### *C. Factors Affecting Battery Aging*

In the utilization process of LIBs, besides the external mechanical losses, deliverable internal chemical reactions also contribute a great deal to battery degradation. First of all, side reactions can result in the growth of the internal resistance, the decrease of the capacity and the power fade which, in its turn, affects the battery aging process. The research of battery out-of-date mechanisms is made more difficult by the complex coupling relationship between these side reactions, which typically do not occur independently [18]. Loss of lithium inventory (LLI), loss of active material (LAM), and rise in internal resistance (IR) are the three main categories used to describe the internal aging process of LIBs. Among them, LAM is primarily caused by the degradation of active particles, which can result from current collector corrosion, adhesive decomposition, transition metal dissolution, or electrode particle cracking. LLI is mainly due to the breakdown and reformation of solid electrolyte interface (SEI) films, electrolyte decomposition, and lithium plating [19]. The factors affecting battery aging and their corresponding types are shown in Fig. 2.

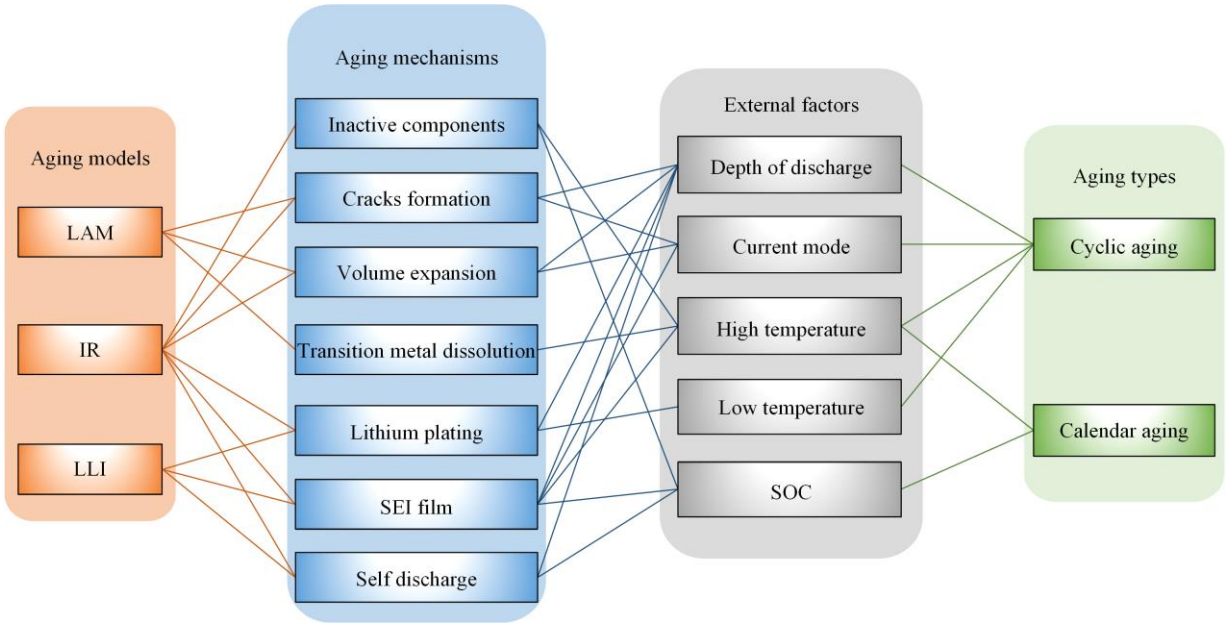


Fig. 2. The factors affecting battery aging and their corresponding type.

## III. Acquisition of Battery Aging Dataset

The aging data of batteries are dominant for battery health prediction studies. However, acquiring a substantial volume of data demands considerable human resources, material, and financial resources. In addition, data quality is also influenced by operations and equipment, and has a significant impact on experimental results. The three commonly used open-source datasets for LIBs are NASA, the University of Maryland CALCE, and the MIT Stanford Toyota Research Center Battery Dataset. This section summarizes some popular and recent datasets. Open data and code can help researchers track research easily and enhance the quality of experimental research. A common method for sharing work-related data and code is to provide access links in the supplementary information of published papers [20]–[23], which makes it easy for readers to find. In order to share data, public data-sharing platforms such as Zenodo [22], [23], Mendeley [24], and OSF [25] can be chosen, while personal websites are also popular for sharing research group data [26]–[28]. For code sharing, readers can easily access and share relevant datasets [27]–[29], or choose a public code-sharing platform, such as Github [20]. The detailed information of each dataset is summarized in Table I, which includes battery chemistry and type, degradation trends, bicycle aging overview, and publication year.

TABLE I
Common Datasets for Lithium-ion Batteries

| Data sources | Cathode chemistry | Battery type | Aging configuration file (charging/ discharging) | Degradation trend | Data and code links |
|---|---|---|---|---|---|
| NASA | NCA | Cylindrical shape | CC-CV/CC | Nonlinear | https://ti.arc.nasa.gov/tech/dash/groups/pcoe/prognostic-data-repository/ |
| CALCE | LCO | Bag/Prism | CC-CV/CC | Sublinear/ super-linear | https://web.calce.umd.edu/batteries/data.htm |
| Oxford | NCA | Small bag | CC-CV/ Dynamic + CC-CV/CC | Linear | https://ora.ox.ac.uk/objects/uuid:03ba4b01-Cfed-46d3-9b1a-7d4a7bdf6fac |
| [20] | NCM/ NCA | Ball | CC-CV/CC | Sublinear/ super-linear | https://zenodo.org/record/6405084# . Y3YQ_3bMJEY/ |
| [22] | NCA | Ball | Calendar aging + CC-CV/CC | Linear | https://ora.ox.ac.uk/objects/uuid:de62b5d2-6154-426d-bcbb-30253ddb7d1e |

## IV. SOH Estimation

This paper categorizes LIB health estimation into two key areas: SOH estimation and EOL prediction, based on the distinct objectives of battery health research. SOH estimation can be model based or data-driven based, as shown in Fig. 3. Data-driven approaches for estimating battery SOH typically involve four distinct steps: model creation, feature selection and identification, data collection and cleaning, and performance evaluation [30].

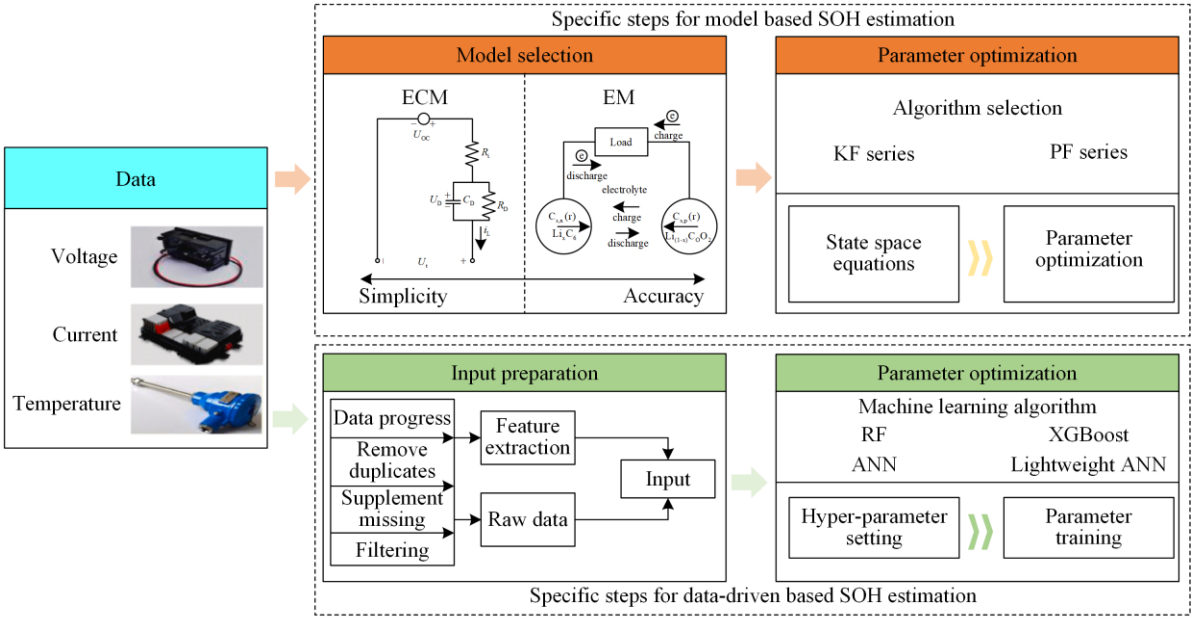


Fig. 3. Approaches for estimating battery SOH and the associated overarching framework.

In battery management, estimation of SOH is very useful as it gives information on present capacity and change in the internal resistance of the battery. This information helps to create enhanced battery control methods that may include decisions on the rate of charging and discharging together with the necessity to plan battery usage and servicing periods more effectively in order to prolong its durability and improve its efficiency. For battery operation, based on real-time data analysis, it is possible to change operating parameters such as charging current in real-time for maximizing the battery utilization rate and safety. In terms of battery control, SOH estimation offers critical feedback to battery management systems, aiding in the implementation of intelligent control strategies. Adjusting control algorithms based on estimated health status enables more precise battery protection and optimization, thereby improving overall system stability and efficiency.

### *A. The Definition of SOH*

Battery capacity retention rate refers to the health state of the battery, and the definition of SOH can be expressed as the degree to which the current performance of the battery deviates from its factory-rated performance, representing the battery's ability to store electrical energy. Many manufacturers stipulate that batteries should no longer be used when their SOH is below 80%, and it is recommended to have them replaced promptly. SOH can be defined according to the following three equations [31], [32]:

$$S_{\mathrm{OH}} = \frac{C_{\mathrm{aged}}}{C_{\mathrm{rated}}} \times 100\% \tag{3}$$

$$S_{\mathrm{OH}} = \frac{Q_{\mathrm{aged(max)}}}{Q_{\mathrm{new(max)}}} \times 100\% \tag{4}$$

$$S_{\mathrm{OH}} = \frac{R_{\mathrm{EOL}} - R_{\mathrm{NOW}}}{R_{\mathrm{EOL}} - R_{\mathrm{BOL}}} \times 100\% \tag{5}$$

where $C_{\mathrm{aged}}$ represents the current capacity; $C_{\mathrm{rated}}$ represents the rated capacity; $Q_{\mathrm{aged(max)}}$ represents the current maximum battery discharge capacity; and $Q_{\mathrm{new(max)}}$ represents the maximum discharge capacity of new battery; $R_{\mathrm{EOL}}$ represents the internal resistance at the end of battery life; $R_{\mathrm{NOW}}$ represents the internal resistance of current battery; and $R_{\mathrm{BOL}}$ represents the new battery internal resistance. The classifications of the 3 different definitions of SOH are provided in Table II.

TABLE II
CLASSIFICATION OF DIFFERENT DEFINITIONS OF SOH

| Equation | Type | Characteristic | Usage frequency |
|---|---|---|---|
| $S_{\mathrm{OH}} = \frac{C_{\mathrm{aged}}}{C_{\mathrm{rated}}} \times 100\%$ | Capacity | Simple | High |
| $S_{\mathrm{OH}} = \frac{Q_{\mathrm{aged(max)}}}{Q_{\mathrm{new(max)}}} \times 100\%$ | Power | The discharge capacity of the battery is considered | Medium |
| $S_{\mathrm{OH}} = \frac{R_{\mathrm{EOL}} - R_{\mathrm{NOW}}}{R_{\mathrm{EOL}} - R_{\mathrm{BOL}}} \times 100\%$ | Impedance | Low accuracy | Low |

### *B. Model Based SOH Estimation Method*

Model based SOH estimation methods typically integrate representative models and parameter estimation algorithms to estimate SOH, as shown in Fig. 4. Existing models are typically divided into equivalent circuit models (ECM) and electrochemical models (EM) [33]. The most mature and popular parameter optimization methods based on models include Kalman filters (KF), particle filters (PF), and their variants [34].

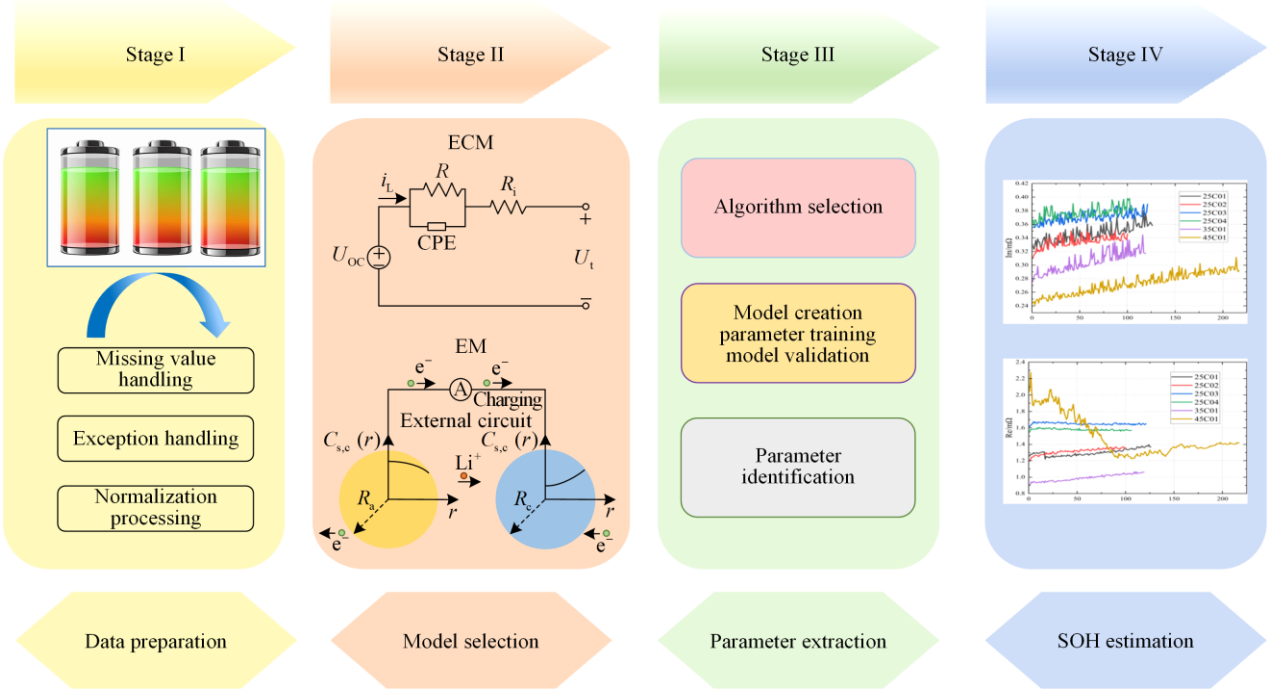


Fig. 4. Step structure for model-based SOH estimation.

#### *1) ECM Methods*

ECM relies on the electrical properties of LIBs, and can be used to analyze the dynamic properties of LIBs. According to the different methods for identifying model parameters, ECM models are categorized into time-domain ECM models and frequency-domain ECM models. The time-domain models encompass the Rint model [35], Thevenin model [36], bipolar model [37], fractional order model [38], as schematically shown in Fig. 5. The frequency-domain model typically refers to the electrochemical impedance spectroscopy (EIS) model [39], [40].

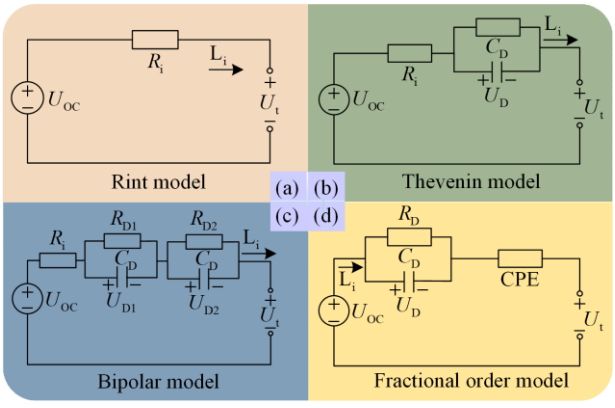


Fig. 5. Common ECM models. (a) Rint model. (b) Thevenin model. (c) Bipolar model. (d) Fractional order model.

Currently, the health assessment of LIBs based on EIS is a hot research topic, and ECM is often used [41]. Reference [42] uses the integer order mode (IOM) for modeling. By adjusting the predicted equivalent series resistance (ESR), charge transfer resistance ($R_{ct}$), and solid-electrolyte interphase resistance ($R_{SEI}$) of the battery and analyzing them using artificial neural networks, it achieves error percentages of 5%, 1.5% and 1% for ESR, $R_{SEI}$ and $R_{ct}$, respectively. The study also shows that the main drawback of IOM is the inability to match the low-frequency region of battery impedance in the frequency domain using integer order ECM. In contrast, fractional order forms (FOM) can better showcase the properties of batteries. Reference [43] proposes FOM of Thevenin and partnership for a new generation of vehicles (PNGV) models based on IOM, employing the extended Kalman filter (EKF) for estimation, with an estimation error of under 0.5%.

In model-based SOH estimation methods, the ECM model has good physical interpretability, with fewer parameters and less computational burden. However, its applicability is poor in high current and low temperature environment. The robustness and generalization ability of ECM based methods are also low, making it difficult to adapt to different types of batteries. Therefore, its application in the real world poses significant challenges.

*2) EM Methods*

The electrochemical model is based on porous electrode theory and concentration dynamics, employing physical equations to numerically describe the electrochemical reaction kinetics, mass transfer, and other microscopic processes occurring within the battery [44]. It elucidates the charging and discharging behavior inside the battery from the principle of electrochemical reaction, and is a typical physical model. EM models, together with LLI, LAM, and IR, are used to describe the battery aging and estimate SOH [45]. EM model also better reflects the internal operating state of the battery. However, while offering high accuracy and high physical interpretability, it necessitates extensive computational resources. It is difficult to implement, so various simplified models, such as the single particle model (SPM), are widely used in SOH estimation because of their reduced computational complexity while retaining high accuracy. The existing commonly used EM methods mainly include the pseudo-two-dimensional (P2D) models type, single particle (SP) models, and various simplified P2D models. Figure 6 shows the reaction mechanism and EM of LIBs of the P2D and SP models.

Reference [46] proposes a LIB estimation capacity fading model based on decreasing current, double correlation analysis, and gated recursive unit (GRU), and verifies its adaptability. Reference [47] simplifies the model by linearizing the coupled partial differential equations of the P2D model and deriving the Laplace transfer function, achieving high approximation accuracy. In [48], a fractional order model is proposed that considers electrolyte polarization and aging mechanisms, achieving accurate voltage estimation and SOH estimation. The computation time of this type of model is 60 times faster than that of the P2D model.

The EM model can still be applicable in extreme situations and has high computational accuracy, but its calibration parameters are difficult and has significant computational difficulties.

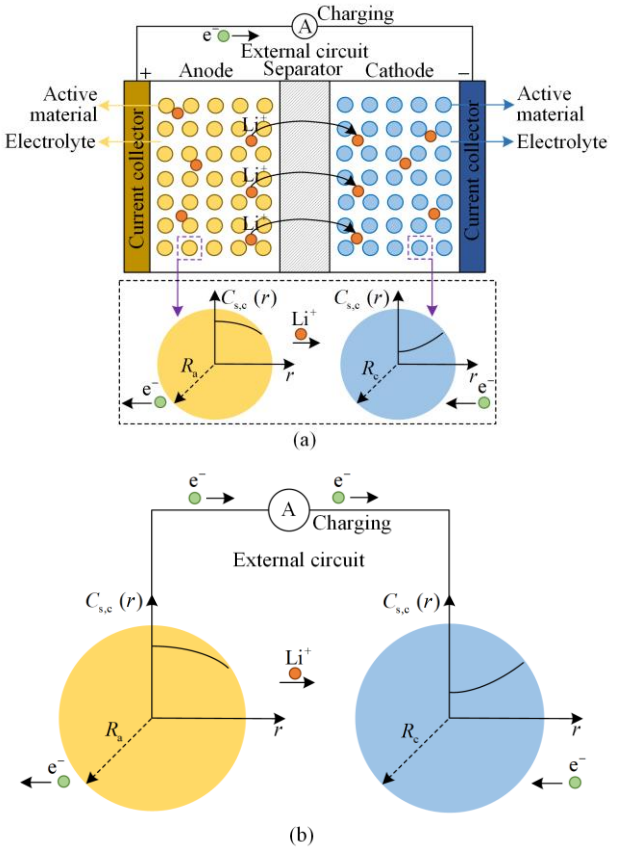


Note: $r$ represents the index of the on-site degradation data. $r$ is used to indicate the degradation data index of lithium-ion batteries at different time points or operational cycles, tracking the variation of SOH over time or cycle count

Fig. 6. Reaction mechanism and EM of LIBs. (a) P2D model. (b) SP model.

Table III provides a summary of the five modelling methods applied in battery SOH estimation.

TABLE III
SUMMARY OF FIVE MODEL METHODS APPLIED IN BATTERY SOH ESTIMATION

| Approach | Battery type | Error percentage (%) | Temperature (°C) | Complexity |
|---|---|---|---|---|
| IOM/ECM [42] | Panasonic NCR 18650B | < 5 | 25 | *** |
| FOM/ECM [43] | Lithium-ion polymer battery | < 2 | 25 | ** |
| GRU/EM [46] | Neware BTS 4000 | < 5 | 25 | ** |
| P2D/EM [47] | intercalation-type cell battery | < 5 | 25 | *** |
| EM [48] | LMO battery | < 5 | 25 | ** |

*3) The KF*

KF can be divided into linear Kalman filters (LKF) and nonlinear Kalman filters (NLKF). Figure 7 shows a detailed classification of KF.

The workflow of LKF can be summarized as initialization, state estimation, and state correction. KF initialization starts with the best available information on the average initial state and error covariance, shown as:

$$\overline{x_0} = E\left[x_0\right] \tag{6}$$

$$\boldsymbol{P}_0 = E\left[\left(x_0 - \overline{x_0}\right)\left(x_0 - \overline{x_0}\right)^T\right] \tag{7}$$

where the average value of the initial state is $x_0$; the error covariance is $\boldsymbol{P}_0$, which is a random vector. The error covariance matrix implies the uncertainty of state estimation and can be used to generate error boundaries. After initialization, before considering any system measurements $y_k$, KF estimates the current state $\overline{x_k}^-$

using the state vector $(\boldsymbol{k}-1)$ from the previous time step, and then calculates the error covariance matrix $(\boldsymbol{P}_k^-)$, as well as the Kalman gain matrix $(\boldsymbol{K}_k)$ as follows:

$$\overline{x_k}^- = A_{k-1}\overline{x_{k-1}}^+ + B_{k-1}u_{k-1} \tag{8}$$

$$\boldsymbol{P}_k^- = \boldsymbol{A}_{k-1}\boldsymbol{P}_{k-1}^+\boldsymbol{A}_{k-1}^{\mathrm{T}} + \boldsymbol{Q} \tag{9}$$

$$\boldsymbol{K}_k = \boldsymbol{P}_k^-\boldsymbol{C}_k^{\mathrm{T}}\left(\left[\boldsymbol{P}_{k/k-1}^-\boldsymbol{C}_k\boldsymbol{C}_k^{\mathrm{T}} + \sum s\right]\right)^{-1} \tag{10}$$

where the Kalman gain matrix weights are innovated to update the state. For example, if $\boldsymbol{P}_k^-$ is big and $\boldsymbol{K}_k$ is often very large, it will forcibly generate large updates, and vice versa. A large measurement noise $s_k$ reduces $\boldsymbol{K}_k$, and it is updated accordingly to be smaller. In the covariance matrix, $\boldsymbol{A}_{k-1}\boldsymbol{P}_{k-1}^+\boldsymbol{A}_{k-1}^{\mathrm{T}}$ partially reduces uncertainty, whereas the other part always increases uncertainty. $\boldsymbol{Q}$ represents the process noise covariance matrix; $\boldsymbol{C}_k^{\mathrm{T}}$ refers to the observation matrix, which maps the system's state vector to the observation space; $\sum s$ refers to the measurement noise covariance matrix. System output $\overline{y_k}$ is related to $\overline{x_k}^-$ as:

$$\overline{y_k} = \boldsymbol{C}_k\overline{x_k}^- + K_k e_k \tag{11}$$

The difference between voltage $\overline{y_k}$ and measured voltage $y_k$ is estimated, known as the error at the battery terminal $e_k$. Errors are fed into the correction state, and the correction state of the error covariance matrix $\overline{x_k}^+$ and $P_{k/k}^+$ have the following relationship:

$$\overline{x_k}^+ = \overline{x_k}^- + K_k e_k \tag{12}$$

$$P_{k/k}^+ = P_k^-(I - \boldsymbol{C}_k K_k) \tag{13}$$

where $K_k e_k$ is called a weighted correction factor. Errors exist due to inaccurate state estimation, inaccurate unit models, or measurement noise in the predicted state, implying new data in the estimation. Hence, the chain of differences is often referred to as the innovation process. When the innovation scale is large, their respective state updates are also large, and vice versa. The nonlinear conversion and measurement functions of NLKF can be written as:

$$f(x_k) = \begin{bmatrix} 1 & 0 & 0 \\ 0 & T^* & 0 \\ 0 & 0 & S^* \end{bmatrix}\begin{bmatrix} S_{\mathrm{OC}_k} \\ V_{\mathrm{RC},f,k} \\ V_{\mathrm{RC},s,k} \end{bmatrix} + \begin{bmatrix} \dfrac{-\eta \mathrm{d}t}{C_N} & 0 & 0 \\ 0 & X^* & 0 \\ 0 & 0 & Y^* \end{bmatrix}\begin{bmatrix} I_{b,k} \\ I_{b,k} \\ I_{b,k} \end{bmatrix} \tag{14}$$

$$g(x_k) = V_{b,k} = V_{\mathrm{OCV}}(S_{\mathrm{OC}_k}) - V_{\mathrm{RC},f,k}(S_{\mathrm{OC}_k}) - V_{\mathrm{RC},s,k}(S_{\mathrm{OC}_k}) - I_{b,k}R_s \tag{15}$$

where $T^*$ and $S^*$ represent $\exp\left(\dfrac{-\mathrm{d}t}{\tau_1(S_{\mathrm{OC}})}\right)$ and $\exp\left(\dfrac{-\mathrm{d}t}{\tau_2(S_{\mathrm{OC}})}\right)$, respectively, while $X^*$ and $Y^*$ represent $(1-T^*)(S_{\mathrm{OC}})R_1$ and $(1-T^*)(S_{\mathrm{OC}})R_2$, respectively; $V_{\mathrm{RC},s,k}(S_{\mathrm{OC}_k})$ is the fast component of transient voltage caused by the first and second RC networks; while $V_{\mathrm{RC},s,k}$ is the slow component of transient voltage caused by the first and second RC networks [49].

Due to their variety, Kalman filters and their variants can solve complex mathematical modeling problems caused by the variation of battery parameters with temperature.

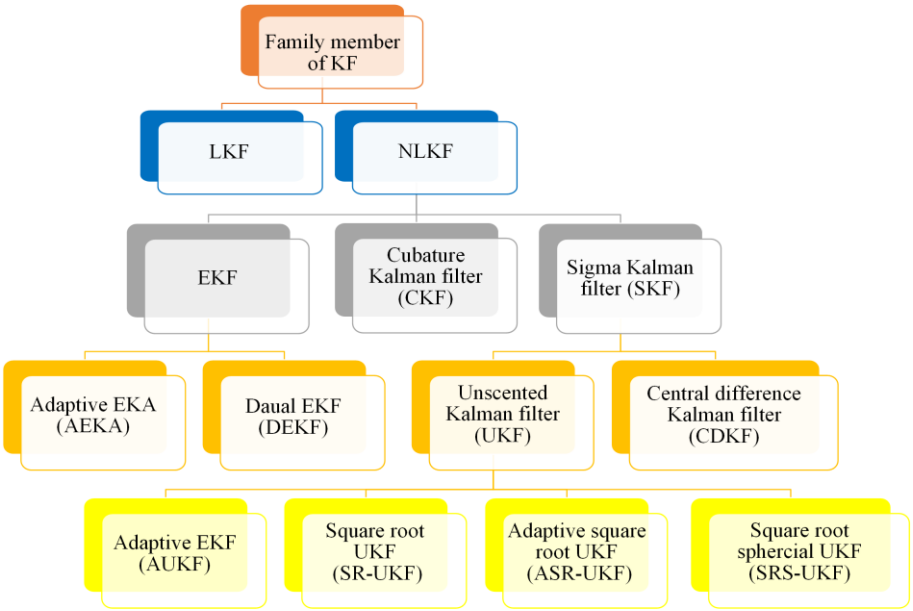


Fig. 7. Schematic diagram of Kalman Filter and its variants.

*4) The Particle Filters*

The standard particle filter (PF) algorithm implements recursive Bayesian filtering using a non-parametric Monte Carlo method [50], which is suitable to describe nonlinear and non-Gaussian systems in state space models [51], [52]. The advantages of the PF algorithm are simple structure and easy implementation. However, particles will experience attenuation and damage during experiment, which will increase the error rate. The process of the PF algorithm is shown in Fig. 8. To improve this method, reference [53] investigates a PF-RLS algorithm that directly optimizes the initial state of PF by increasing the particle density distribution. After obtaining the life cycle parameters of the experimental battery, the least squares method is employed to fit the initial SOH parameters, utilizing these initial parameters as the starting values for PF to produce a refined probability distribution. The maximum root mean square error of this method is 0.78%, and the maximum average absolute error is 1.01%. Reference [54] proposes an ePF algorithm by improving particle mass, reducing particle degradation, and accelerating computation. The degraded particles are replaced with newly generated high-quality particles to generate a better posterior probability density function for PF. The developed ePF-EF framework outperforms other predictors under all testing conditions, and is approximately 55%, 50%, and 13% more accurate than the other filter with estimation starting points at 86, 106, and 126, respectively.

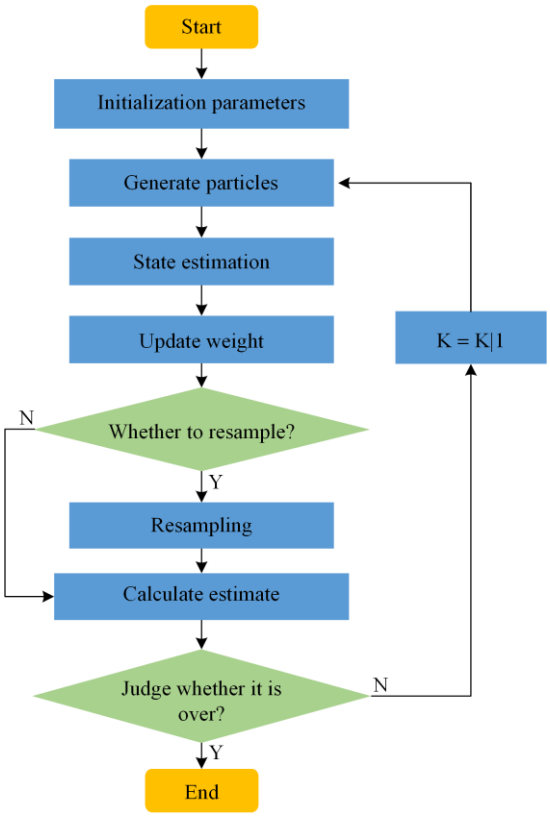


Fig. 8. Particle filter algorithm flowchart.

PF has the same properties as KF, with high computational accuracy and strong physical interpretability. However, it has a heavy computational burden and is difficult to implement in practice.

*C. Data-driven Based SOH Estimation*

The above model-based estimation methods mainly rely on establishing models to obtain the property parameters of batteries and reflect their health state, which have good physical interpretability. However, the models have high computational requirement and complexity, making them difficult to apply in practical applications. Based on data-driven methods, a nonlinear relationship between input and output can be established through machine learning. This approach does not need to consider the chemical reactions and reaction principles inside the battery, but requires a large amount of data training to improve estimation accuracy [55]. This type of method is suitable for similar models and requires the research object to be mature products produced in batches.

*1) Random Forest Method*

Random forest (RF) assesses the SOH of LIBs by analyzing voltage, current, and time data obtained during the charging process. The collected primitive data can be immediately input into the trained model without any preprocessing, thereby reducing computational costs. Incremental capacity analysis is used for feature selection. It is an ensemble learning algorithm that originates from decision tree (DT) algorithms, and its weak learner consists of multiple DTs [56]. By randomly sampling the sample set data, a new sample set is constructed. Then, the sample data is input into multiple DTs for training and forming a more powerful model to improve the accuracy of model estimation [57]. The schematic diagram of the RF model is shown in Fig. 9. In the study using RF, charging and discharging experiments are conducted on batteries, and the feature variables are extracted. The outlined steps include:

1) Generating a new training set through random sampling from the original dataset.

2) Random selection of feature vectors is carried out from ten feature vectors at every node of each tree, with the optimal split determined by minimizing the squared error.

3) Step 2) is iterated until no tree is grown. Pruning algorithms are not required during the growth process of each tree.

RF demonstrates robust data mining capabilities, delivering highly accurate estimation outcomes with strong interpretability [58]. In specific application scenarios, RF models exhibit superior estimation accuracy compared to machine learning models, such as DT [59], CNN [60], and long term short term memory neural networks (LSTM) [61]. In addition, RF models exhibit

higher estimation accuracy in certain applications scenarios [62], [63].

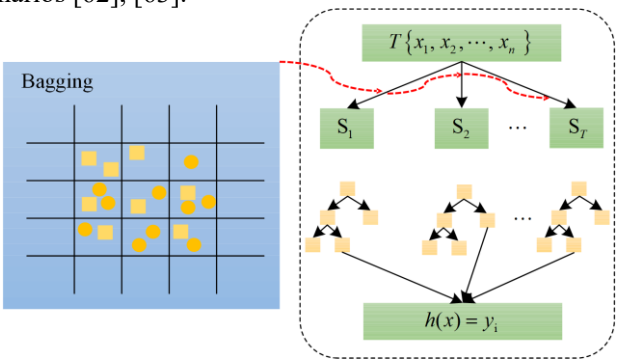


Fig. 9. Random forest working diagram.

*2) XGBoost Method*

XGBoost is an efficient and advanced algorithm built on the gradient boosting decision tree (GBDT) framework, incorporating both linear scaling and decision tree learning. Unlike traditional boosting libraries, XGBoost employs second-order Taylor expansions of the loss function and integrates two regularization terms, L1 and L2, to identify the overall optimal solution. This approach evaluates both reductions in the objective function and the overall complexity of the model, significantly enhancing model's generalization capabilities [64]. Figure 10 shows the structure of XGBoost.

Assuming the experimental dataset for estimating LIB parameters is represented by $E$, given as $E=\{(\alpha_i,\beta_i): i=1,2,\cdots,n;\ \alpha_i \in R_p;\ \beta_i \in R\}$, it consists of $p$ features from the aggregate of $n$ samples, including voltage, current, temperature, charge, etc. Assuming that a regression tree of $m$ $(m=1,2,\cdots,M)$ is given, and $G$ is the set space of the regression tree, the model can be represented as:

$$\overline{\beta_1} = \sum_{m=1}^{M} f_m \alpha_1, f_m \in G \tag{16}$$

The target function is:

$$F_{\text{obj}} = \sum_{i=1}^{n} l(\beta_1, \overline{\beta_I}) + \sum_{m=1}^{M} \mu(f_m) \tag{17}$$

where $\overline{\beta_I}$ is the predicted value; $\beta_1$ is the true value; $l$ is a differentiable convex loss function used to measure the difference between predicted and actual values, while $\mu(f_m)$ is a common term added to XGBoost models to prevent overfitting. Finally, it can be concluded that the objective function is a second-order Taylor expansion with typical terms $\mu(f_m)$, given as:

$$f_{\text{obj}}(t) \cong \sum_{i=1}^{n} \begin{bmatrix} \alpha_{\overline{\beta_i}(t-1)} I\left(\beta_i, \overline{\beta_i}^{(t-1)}\right) f_t(\alpha_i) + \\ \frac{1}{2}\alpha^2_{\beta_i(t-1)} I\left(\beta_i, \overline{\beta_i}^{(t-1)}\right) f_t^2(\alpha_i) + \\ \mu(f_m) + \sigma \end{bmatrix} \tag{18}$$

$$\mu(f_m) = \varphi H + \frac{1}{2}\delta \sum \eta^2 \tag{19}$$

where points $\eta$ and $H$ are the leaf weight value and the number of leaf nodes, respectively; $\varphi$ is a leaf weight penalty factor; and due to the iteration of the objective function, $\delta$ is a constant. $\eta^2$ refers to the squared weights of leaf nodes. Reference [20] finds that the root mean square error (RMSE) of the XGBoost method's training and testing decreases with increasing relaxation time, with a test RMSE of only 1.1%.

XGBoost is a scalable tree-boosting machine learning system known for its efficient learning performance and effectiveness. Its model does not exhibit sample duplication during sampling, and XGBoost supports subsampling and column sampling. Subsampling reduces overfitting by not using the complete samples in each round of calculation. Column sampling randomly extracts a certain proportion of features calculated in each round for training, thus improving speed and reducing overfitting [65], [66]. However, XGBoost is quite sensitive to outliers, and any outliers in the data can significantly impact the training and prediction results of the model. Additionally, XGBoost tends to overfit when dealing with small amounts of data, hence requiring sufficiently large datasets to train the model for accurate prediction results.

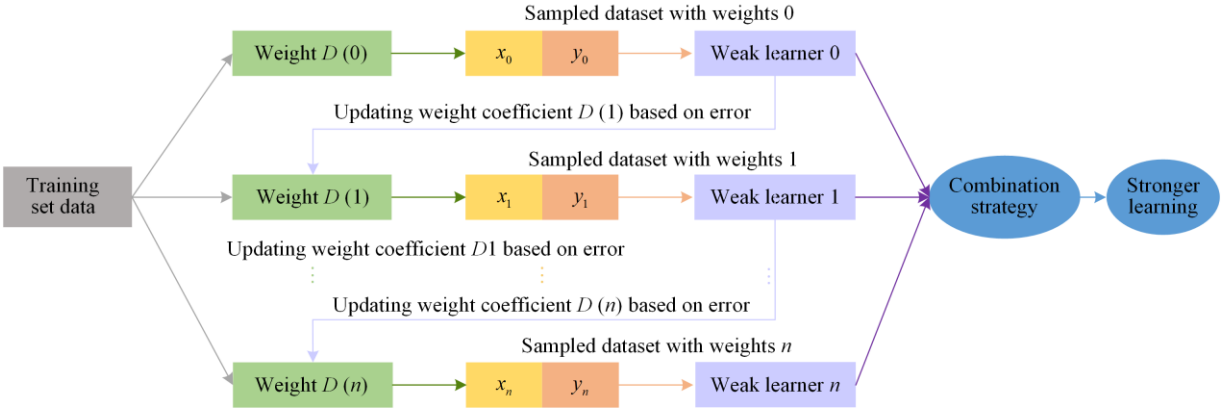


Fig. 10. The structure of XGBoost.

*3) Artificial Neural Network Method*

In the probabilistic machine learning based methods for the estimation of SOH of LIBs mentioned above, manual feature extraction is required for input, which often has poor generalization and accuracy. Implementing automatic feature extractions in data-driven models requires strong nonlinear properties so deep learning techniques are most suitable. Multilayer auto-encoders and decoders are very popular in automatic feature extraction.

Artificial neural networks can be classified into three categories based on their architecture: ANN, recurrent neural network (RNN), and convolutional neural network (CNN) [67]. Figures 11(a) and (b) show the structures of ANN and RNN, respectively. Neural networks can adapt to any nonlinear regression task [68]. Reference [69] is the first that introduces the concept of artificial neural networks, where artificial neurons also have an input layer and an output layer. In [70], the SOH estimation framework is proposed, which combines mixers and bidirectional time convolutional neural networks, to maximize the utilization of local and global characteristics of input features for estimation, with RMSE kept within 2.34%.

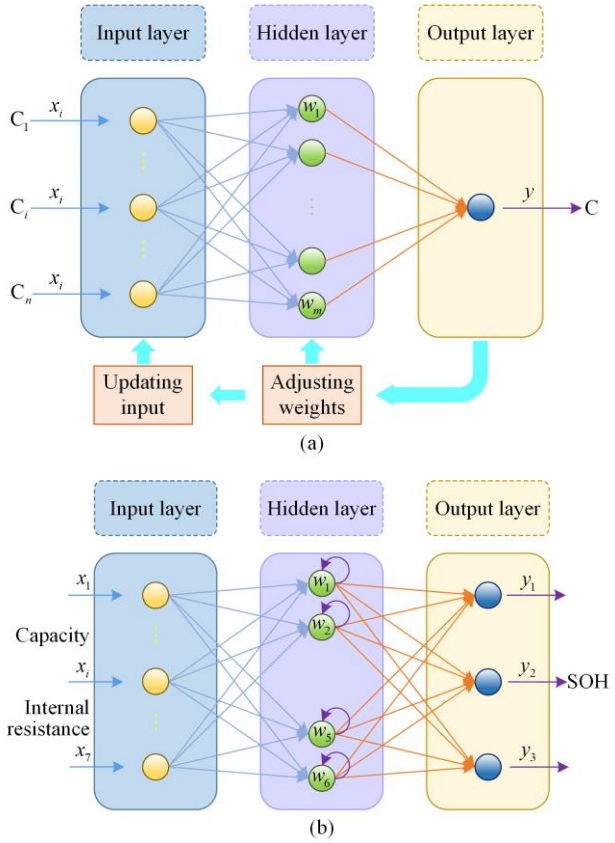


Fig. 11. The structure of ANN. (a) ANN structure. (b) RNN structure.

Table IV summarizes the two data-driven methods applied in battery SOH estimation.

TABLE IV
SUMMARY OF TWO DATA-DRIVEN METHODS APPLIED IN BATTERY SOH ESTIMATION

| Approach | Battery type | RMSE (%) | Temperature (℃) | Complexity |
|---|---|---|---|---|
| XGBoost [20] | NCA, NCM and NCM+NCA | 1.1 | 25, 35 and 45 | *** |
| ANN [70] | NCA | < 2.34 | 25 | ** |

Research on lightweight neural networks is one of the hot topics at present. The main properties of lightweight neural networks are small model size and short computation time. They can be divided into the Mobilenet model and the ShuffleNet model, as Fig. 12 shows the architecture comparison of the two.

MobileNet: MobileNet V1 is the first CNN model proposed by Google for mobile networks, while MobileNet V2 is an improvement on MobileNet V1. The main idea of MobileNet V1 is to use depthwise separable convolution (DepSep Conv). If the computation of standard convolution is HWNK2M, the computation of DepSep Conv is:

$$HWNK^2(\text{depthwise}) + HWNM(\text{pointwise}) = HWN(K^2 + M) \tag{20}$$

where $H$ and $W$ represent the height and width of the input feature map, respectively; $N$ and $M$ denote the number of output channels and input channels, respectively; $K$ and $M$ refer to the kernel size and the width of the layer, respectively.

$$\frac{\text{depthwise+pointwise}}{\text{conv}} = \frac{(K^2+M)HWN}{K^2MHWN} = \frac{1}{K^2} + \frac{1}{M} \tag{21}$$

In order to minimize Mobilenet V1's computation load, the numbers of input and output feature channels, $M$ and $N$, are multiplied by the width factor $\alpha(\alpha \in (0,1))$, which has typical values of 0.25, 0.5 and 0.75, and the total computation amount of depth-separable convolution can be further minimized to:

$$HWK^2 \cdot \alpha M + HW \cdot \alpha N \cdot \alpha M \tag{22}$$

where $\alpha$ is a scaling factor that adjusts the network size, typically ranging between 0.25 and 0.75.

Too many convolutional layers can lead to gradient dispersion, so skip connections are added based on MobileNet V1 to provide functional reuse during forward propagation. At the same time, MobileNet V2 also uses point-to-point convolution to enhance dimensionality.

ShuffleNet: The key operation in the ShuffleNet V1 block is the channel shuffle layer, which alters the channel sequence between two consecutive convolutions. Channel shuffle implements the information exchange mechanism of packet convolution, which can greatly reduce the computational workload.

Based on ShuffleNet V1, ShuffeNet V2, proposed by Face++, uses direct indicators (computing speed) rather than indirect evaluation indicators. ShuffeNet V2 uses different input and output channel widths and makes

element-level operations, which increase the amount of convolution. At the same time, its multiple branches reduce operational efficiency. Figure 12 shows the architecture comparison of MobileNet and ShuffleNet.

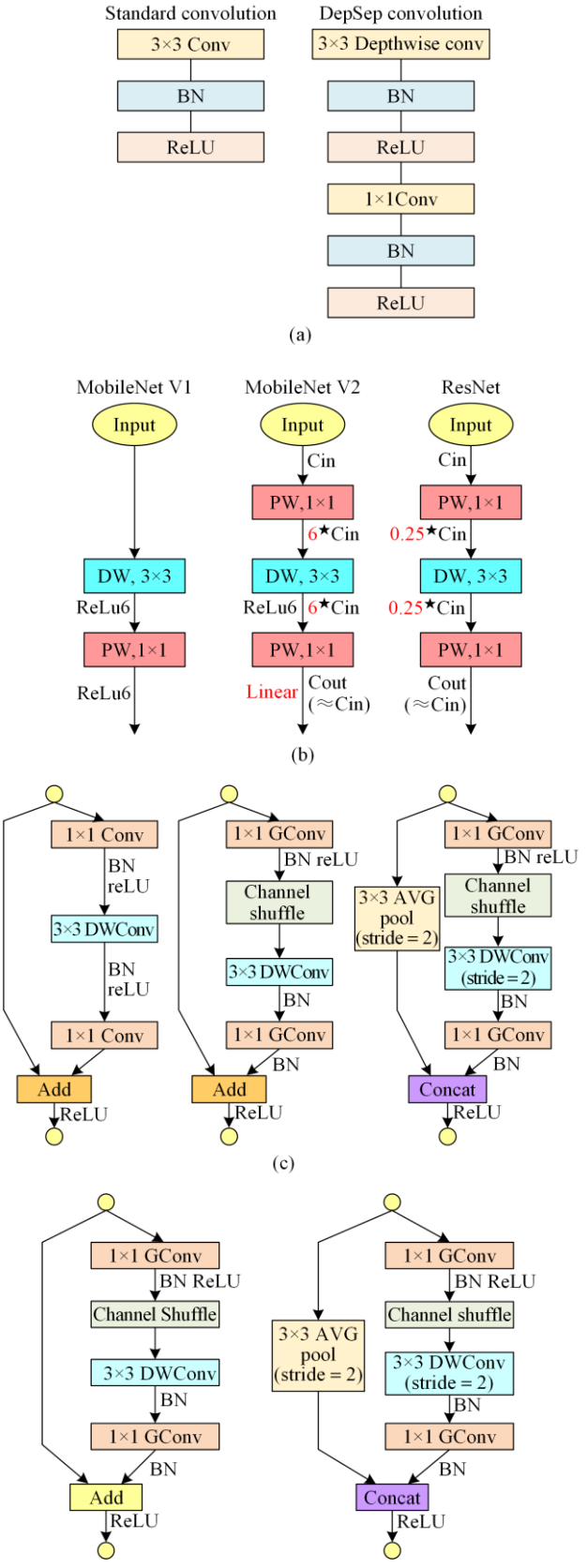


Fig. 12. Architecture comparison of MobileNet and ShuffleNet. (a) Comparison of conventional convolutional architectures versus deep and separable convolutional architectures. (b) Architecture comparison of Mobile V1, Mobile V2, and ResNet. (c) Shuffle V1 Block architecture. (d) The fundamental unit of ShuffleNet V2, ShuffleNet V2 unit for spatial downsampling (2×), ShuffleNet basic unit, and ShuffleNet cells for spatial downsampling (2×) are the building elements of ShuffleNet V1 still arranged from left to right referring to [71] with permission.

ANN excels in capturing intricate nonlinear relationships from data, rendering them exceptionally versatile for managing intricate lithium-ion battery data. Parallel processing capabilities enable ANNs to expedite both model training and prediction procedures through parallel computation, a feature particularly advantageous for extensive datasets. However, the extensive computational resources and time that are often necessary for training ANNs on large-scale datasets, especially when dealing with complex network structures, present a notable challenge. Additionally, the inherent complexity of ANNs, resulting in black-box models, poses difficulties in explaining the decision-making process and diminishes interpretability.

Table V provides an overall evaluation of the SOH estimation methods.

TABLE V
EVALUATION OF SOH ESTIMATION METHODS

| Objective | Methodology | Advantages | Disadvantages |
|---|---|---|---|
| SOH estimation | ECM | High physical interpretability fewer parameters low computational burden | Poor in high current poor in low-temperature |
| | EM | Robustness under extreme conditions high accuracy | High computational burden difficult to calibrate parameters |
| | KF | Solving complex problems | Poor stability |
| | PF | High accuracy | High computational burden |
| | RF | High accuracy Fewer parameters | Unable to fully utilize all parameters |
| | XGBoost | Efficient learning performance strong generalization ability | Sensitive to outliers large data requirements |
| | ANN | High accuracy | Low interpretability |

## V. EOL Prediction Method

Long-term prediction of battery lifespan is referred to as EOL prediction. Most recent investigations in EOL prediction rely mainly on data-driven methods. As a result, this paper divides data-driven EOL prediction methods into two categories based on the necessity for feature extraction: feature-based and deep learning methods, as shown in Fig. 13.

For battery planning, EOL prediction uses current degradation rates and usage patterns to forecast when the battery is likely to reach the end of its usable life. This allows for advanced scheduling of replacement plans and anticipation of maintenance needs, thereby optimizing resource allocation. In terms of battery operation, predicting when the battery is nearing the end of its life enables adjustments in operational decisions to extend its lifespan and ensure safety. Regarding battery control, integrating EOL prediction with battery management systems enhances control strategies. This involves early warning systems and adaptive control algorithms that adjust parameters based on predicted remaining life, as so to optimize performance and reliability throughout the battery's entire lifecycle.

The key difference between EOL prediction and SOH estimation methods lies in the fact that each battery has only one EOL point. As a result, large datasets of batteries that have aged to their EOL are necessary for accurate data acquisition and modeling in EOL prediction. This type of prediction develops relatively slowly because of the difficulty in obtaining data, and there are also much fewer EOL prediction approaches.

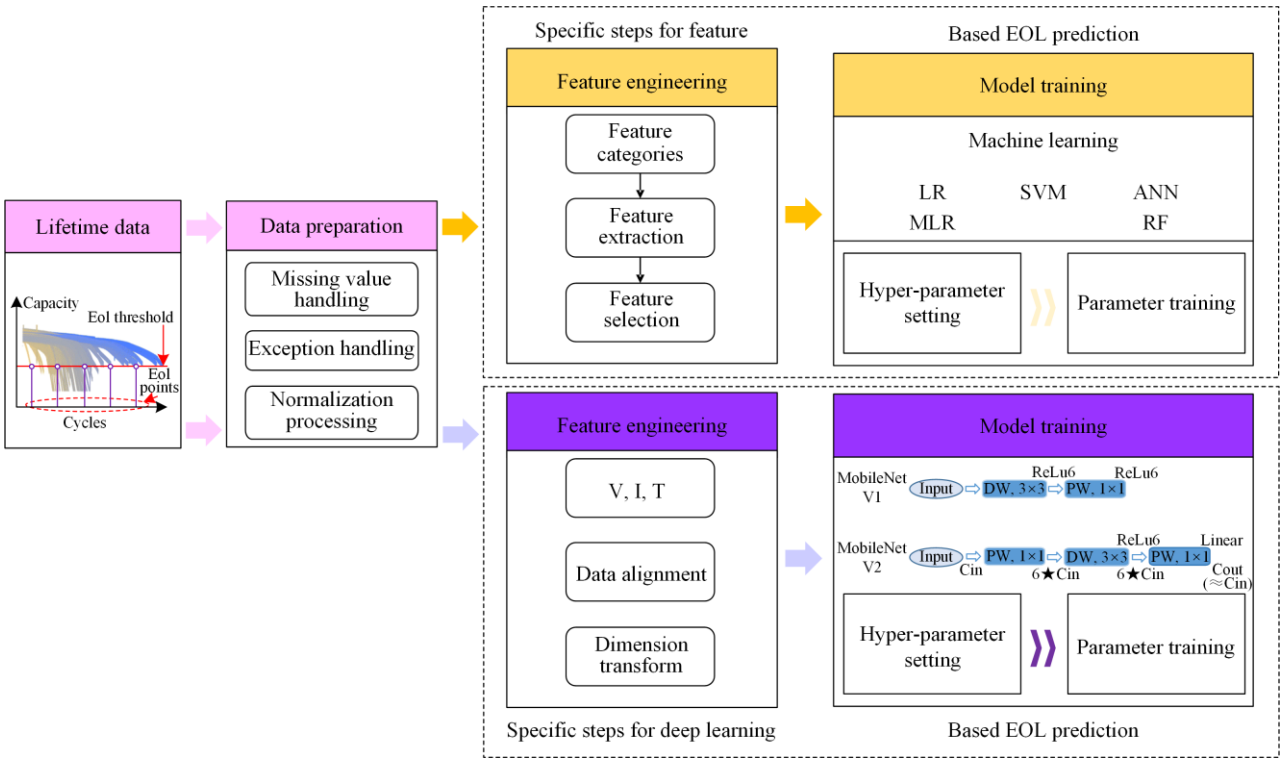


Fig. 13. Approaches for predicting battery EOL and the associated overarching framework.

### A. Feature Based EOL Prediction Method

The fundamental concept of this approach involves extracting features from the current, voltage, capacity, and temperature profiles, and subsequently employing machine learning [72] algorithms to establish the relationship between these features and battery longevity. This method can be summarized into the following four steps, as schematically shown in Fig. 14. The first step is to conduct charging and discharging experiments on large numbers of batteries to obtain battery data and extract various features based on the aging correlation analysis of parameters. There are currently popular feature extraction methods based on voltage, current, internal resistance, capacity, and temperature. Due to the low correlation between many features, in the second step, the optimal subset of features are selected, with the more prevalent methods being filter-based, wrapper-based, embedded-based, and fusion-based techniques. The third step is to match the representation between the selected function and battery life through various machine learning algorithms, while for the final step, the fitting model is evaluated through testing the dataset. From the prediction steps of EOL, we can see that the EOL prediction and SOH estimation processes are similar, but they reflect different relationships. SOH estimation maps the relationship between the properties of each cycle and SOH. In contrast, EOL prediction seeks to establish the relationship between battery aging characteristics under similar operating conditions and EOL.

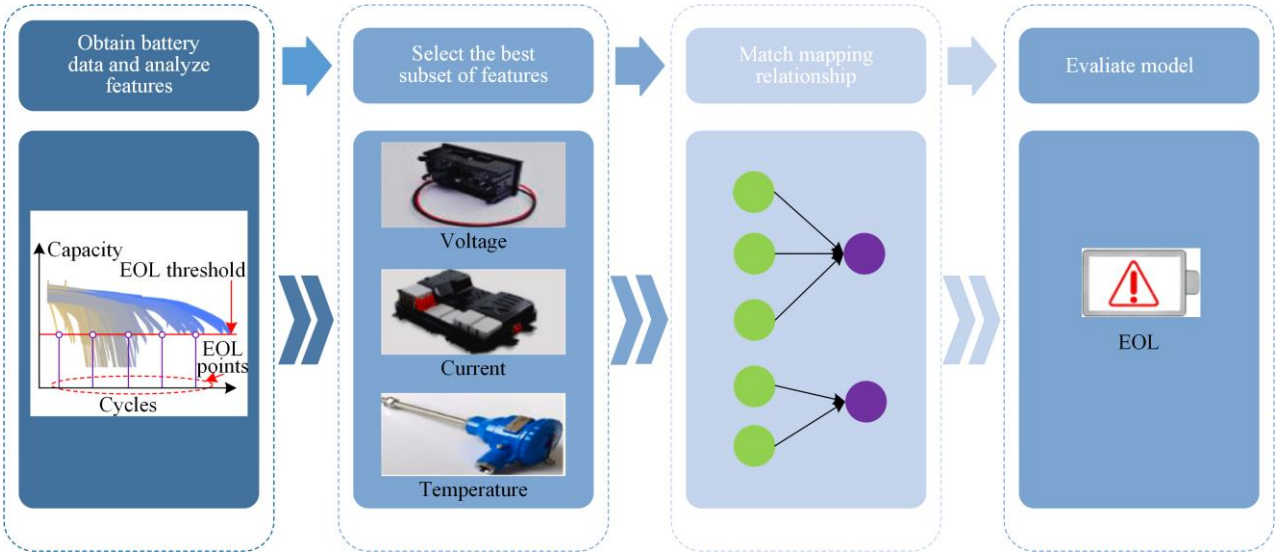


Fig. 14. Flow chart of EOL prediction method based on features.

Reference [73] proposes a hybrid framework for predicting EOL for batteries and assessing uncertainty, utilizing Gaussian process regression (GPR) and KF. A hybrid method combining empirical mode decomposition (EMD) and PF is also adopted. In large numbers of end-of-life cycle tests, it was found that the standard deviations of the four batteries selected in the experiment have decreased by 68%, 46%, 70%, and 65%, respectively. Reference [74] presents a novel extended kalman particle filter (EKPF) algorithm, refining the EKPF approach by integrating EKF as the density sampling function, with all experimental errors falling under 5%. Table VI summarizes the two described feature methods applied in battery EOL prediction.

The feature-based method entails manual feature extraction, with the correlation between features and the EOL point bolstering the interpretability of this approach. Its advantage lies in not necessitating abundant data or intricate model construction, thereby broadening its applicability and enhancing computational efficiency. Nevertheless, this method heavily depends on features, and the caliber of features markedly influences result accuracy. Furthermore, it may not be suitable for certain nonlinear models.

TABLE VI
SUMMARY OF TWO METHODS APPLIED IN BATTERY EOL PREDICTION

| Type | Battery type | RMSE | Temperature (°C) | Complexity |
|---|---|---|---|---|
| Feature based [73] | NCA | Not mentioned | 25 | ** |
| Feature based [74] | NBT5V10AC16-T battery | $<$ 5% | 25 | *** |

### *B. Deep Learning Based EOL Prediction Method*

Deep learning methods effectively capture the nonlinear relationships associated with LIB EOL in a feature-agnostic manner [75]. The feature based EOL prediction method requires manual feature extraction, which reduces the accuracy of the experimental results. Deep learning is a method of constructing multi-layer or deep neural networks, which solve the problems of supervised classification, modeling, or reinforcement learning [76]. The EOL prediction method is based on deep learning and attempts to use neural networks to obtain data automatically. Figure 15 shows a typical framework for battery EOL prediction using deep learning [34].

Reference [77] also proposes a regression model based on manually selected features to predict EOL, using discharge data from the first 100 cycles, achieving a 9.1% relative average absolute percentage error of EOL. Subsequently, reference [29] optimizes the closed-loop fast-charging protocol using the same regression model and generates more LIB cell data with more complex fast-charging strategies. In [78], a CNN model is developed and applied to the same dataset, successfully reducing the input data required for continuous charging cycles to 20 while maintaining accuracy.

The deep learning approach addresses certain limitations of feature-based methods by autonomously capturing intricate patterns and features within the data, rendering it applicable to issues characterized by highly nonlinear relationships. Based on multilayer structure, deep learning models are good at handling big amounts of data, identifying functional dependencies and demonstrating a high degree of versatility in tasks solving. Nevertheless, this approach demands considerable data resources, which may result in overfitting or subpar outcomes.

Table VII provides an evaluation of the described EOL prediction methods.

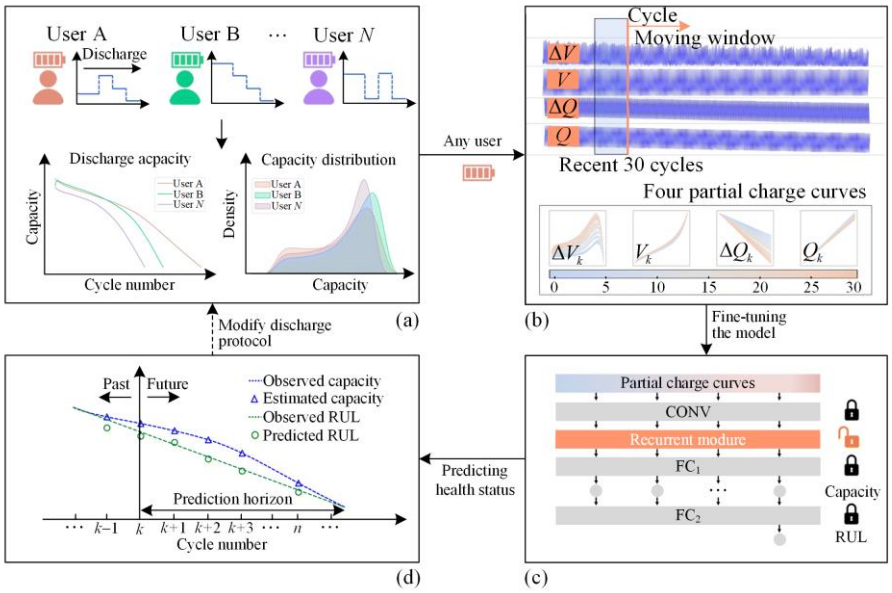


Fig. 15. Typical framework for battery EOL prediction using deep learning referring to [34] with permission.

TABLE VII
EVALUATION OF EOL PREDICTION METHODS

| Objective | Methodology | Advantages | Disadvantages |
|---|---|---|---|
| EOL prediction | Based on feature | Early prediction<br>Low computational burden | Large requirement of experiments<br>Difficult to find suitable features |
| | Based on deep learning | High accuracy in early prediction<br>Good generalization | High computational burden<br>Poor interpretability |

## VI. FUTURE DEVELOPMENT TRENDS AND MAIN CHALLENGES

Battery health management has become a hot research topic recently. While different prediction methods can address various real-world battery problems, significant challenges remain in this field.

### *A. Challenges Under Extreme Temperatures*

Most experiments conducted by researchers are performed at normal room temperature (25 °C), with relatively limited data available on battery health at temperatures below –20 °C or above 45 °C. However, LIBs are used at extreme temperatures, e.g., geological exploration and daily human life in high-latitude regions, operation of drones and other aircraft in high-temperature environments, etc. At extremely low temperatures, significant changes occur in the chemical reactions of batteries, and models for battery aging and degradation also differ. Moreover, feature extraction of voltage and temperature is affected by low temperatures. Therefore, battery prediction methods at room temperature will no longer be applicable for predictions at extremely low temperatures [79]. High temperature accelerates the rate of chemical reactions, and the decomposition of SEI films and cathode materials, thus increasing the aging rate of batteries. Operating batteries under high-temperature conditions may lead to some potential failures. Hence, conventional prediction models are no longer applicable under extremely high-temperature conditions.

To address this issue, temperature-related features need to be extracted. Initially, internal sensing techniques can be employed to accurately obtain the internal temperature and thermal parameters of the battery. Subsequently, a thermal model can be established to simulate the temperature variations of the battery. Alternatively, machine learning-based approaches can be utilized to extract temperature-related features from the physical properties of lithium-ion batteries, such as the thickness of the SEI film. After extracting temperature-related parameters, electrical characteristic tests and EIS tests of batteries at both room temperature and extreme temperatures can be compared. Features selected through EIS and RF methods, aiming to minimize errors compared to those based on Pearson correlation coefficient (PCC), can be applied to LSTM models. However, extracting general features and temperature-related features that exhibit high elasticity in different aging scenarios poses a challenge and necessitates extensive experimental exploration.

### *B. Challenges of Accurate Prediction at Different Battery Usage Stages*

Batteries go through different states as they are in use and these states are clearly defined. Nevertheless, the developed models are incapable of explaining the var-

ying aging behaviors between these stages. Also, determining the correct stage of aging still presents quite a challenge. Multi-model prediction and model fusion strategies can address this challenge. Multiple sub-models can be constructed to represent the primary degradation modes at various stages, and subsequently, the aging pattern can be identified and the most suitable degradation model can be selected. During phase transitions, the merging of two adjacent models can be employed to ensure a smooth transition. Additionally, multi-model fusion aids in enhancing prediction accuracy and robustness.

Reference [80] introduces a self-supervised learning framework to enhance the accuracy of battery SOH estimation. This approach can predict SOH across various battery chemistries, formats, operating conditions, and environments, achieving an overall error rate of less than 1.14%. However, this approach leads to increased computational costs, and further research is required on pattern recognition and model fusion methods.

### *C. Development Trends Driven by Interdisciplinary Estimation and Storage Optimization*

Interdisciplinary research and technology can significantly drive the development of health prediction for LIBs. In addition to the interdisciplinary research involving machine learning mentioned earlier, advancements in materials science and nanotechnology can greatly enhance the performance of LIBs, improving their resistance to degradation and cycle life, thereby reducing the rate of battery decay and favoring increased prediction accuracy. The future direction of LIB material selection tends toward lower resistance and lower loss rates. Furthermore, the development of sensing technology can also enhance the accuracy of LIB prediction. Real-time monitoring of LIBs under different usage conditions enables a more comprehensive understanding of their status. The trend in sensor development leans toward miniaturization and comprehensive measurement of multiple parameters.

Supercapacitors are key devices in the field of energy storage. Reference [81] introduces a new technology that combines variational mode decomposition (VMD) with bidirectional long short term memory (BiLSTM) neural networks to predict the lifespan of supercapacitors. The average root mean square error measured in the experiment is 0.112 519. By integrating machine learning, materials science, and sensor development, the accuracy of health prediction for LIBs can be further enhanced. Interdisciplinary development and storage optimization are important trends for future development.

### *D. Development Trends of Multi Task Learning*

In existing researches, most single task learning methods adapt data-driven approaches, focusing only on specific measurement tasks, e.g., the measurement of a certain period. However, in practical applications, it is difficult to conclude that a certain cycle can represent better than other cycles. Therefore, multi-task learning can more comprehensively predict the health status of batteries. Compared to independent learning for each task, learning multiple related tasks simultaneously can produce powerful results [82]. The methods of multi-task learning possess enhanced learning and adaptation capabilities, allowing for robust generalization across different data distributions. By integrating multiple objectives or models, multi-task learning can improve prediction accuracy and robustness. Additionally, multi-task learning facilitates interdisciplinary collaboration, offering novel insights for detecting the health of LIBs.

Reference [27] introduces a data-driven prediction framework for multi-task learning to forecast capacity and power degradation. This model effectively predicts capacity, internal resistance, and the degradation trajectory, including knee and end-of-life points during the early stages of battery life. In [83], the long-term degradation trajectory is directly predicted using recursive prediction features under a multi-task framework, achieving a prediction RMSE of less than 2% and a fitting coefficient of greater than 0.86.

## VII. Conclusion

In recent years, considerable attentions have been paid to monitoring and predicting mechanical health within the academic community. The fundamental differences between the health monitoring and prediction of LIBs and mechanical systems arise from the unique nature of the battery system. This paper delves into the methodologies for predicting the health of LIBs. Although model-based methods can accurately represent the aging principle inside batteries and have good physical interpretability, the complexity and multidimensional nature of their parameters make the methods computationally intensive. Their online evaluation and real-time prediction capabilities are also poor, making them difficult to implement in real-world applications. The data-driven approaches eliminate the need to account for internal chemical reactions within batteries, thus offering high accuracy and a broad range of applications. However, their disadvantage is that they overly relies on datasets, and thus, their accuracy is greatly affected by the fluctuations of datasets. A review of numerous recent studies are provided in this paper, although many of the studies are still relatively immature. Nevertheless, the use of sophisticated and innovative methods is considered highly promising for making more accurate estimates of LIB performance. This paper offers useful insights and ideas for researchers exploring the health prediction of LIBs.

## ACKNOWLEDGMENT

Not applicable.

## AUTHORS' CONTRIBUTIONS

Jiahui Ren: building overall framework of the total, making comparative analysis of the state of health (SOH) estimation and end of life (EOL) prediction methods, and the future development directions. Jinkai Ma: editing the literature, preliminary reading and simple analysis. Honghong Wang: creating the charts and visual expressions in the review. Teng Yu: making the operating principle of lithium-ion batteries. Kai Wang: coordinating the entire research work, the key directions of the research, and academic exchanges. All authors read and approved the final manuscript.

## FUNDING

This work is supported by the Youth Innovation Technology Project of Higher School in Shandong Province (No. 2022KJ139).

## AVAILABILITY OF DATA AND MATERIALS

Please contact the corresponding author for data material request.

## DECLARATIONS

Competing interests: The authors declare that they have no known competing financial interests or personal relationships that could have appeared to influence the work reported in this article.

## AUTHORS' INFORMATION

**Jiahui Ren** is currently studying at the School of Electrical Engineering, Qingdao University, Shandong province, China. Her research interests include state assessment and remaining useful life prediction of new energy storage devices and energy storage.

**Jinkai Ma** is currently studying at the School of Electrical Engineering, Qingdao University, Shandong province, China. His research interests include intelligent monitoring of power systems, state of charge and state of health estimation of lithium-sulfur batteries.

**Honghong Wang** works at the School of Electrical Engineering, Qingdao University, Shandong province, China. Her research interests include automatic monitoring of power systems and adaptive intelligent control of complex nonlinear systems.

**Teng Yu** works at the School of Electronic and Information Engineering, Qingdao University, Shandong province, China. His research interests include artificial intelligence, machine learning and computer vision.

**Kai Wang** works at the School of Electrical Engineering, Qingdao University, Shandong province, China. His research interests include state assessment and life prediction of new energy storage devices, energy storage element, storage and conversion of new energy.

## REFERENCES

[1] R. Deng, M. Wang, and H. Yu *et al.*, "Recent advances and applications toward emerging lithium–sulfur batteries: working principles and opportunities," *Energy & Environmental Materials*, vol. 5, no. 3, pp. 777-799, May 2022.

[2] A. R. Bais, D. G. Subhedar, and S. Panchal, "Critical thickness of nano-enhanced RT-42 paraffin based battery thermal management system for electric vehicles: a numerical study," *Journal of Energy Storage*, vol. 52, Aug. 2022.

[3] J. Tian, D. Yang, and X. Zhang *et al.*, "An intelligent charging scheme for lithium-ion batteries of electric vehicles considering internal attenuation modes," *IEEE Journal of Emerging and Selected Topics in Power Electronics*, vol. 12, no. 1, pp. 82-94, Feb. 2024.

[4] Z. Wei, J. Hu, and H. He *et al.*, "Embedded distributed temperature sensing enabled multistate joint observation of smart lithium-ion battery," *IEEE Transactions on Industrial Electronics*, vol. 70, no. 1, pp. 555-565, Jan. 2022.

[5] Y. Che, Y. Zheng, and S. Onori *et al.*, "Increasing generalization capability of battery health estimation using continual learning," *Cell Reports Physical Science*, vol. 4, no. 12, Dec. 2023.

[6] Y. Che, S. B. Vilsen, and J. Meng *et al.*, "Battery health prognostic with sensor-free differential temperature voltammetry reconstruction and capacity estimation based on multi-domain adaptation," *ETransportation*, vol. 17, Apr. 2023.

[7] Q. Zhang, C. Li, and Y. Wu, "Analysis of research and development trend of the battery technology in electric vehicle with the perspective of patent," *Energy Procedia*, vol. 105, pp. 4274-4280, Jun. 2017.

[8] M. Danzer, V. Liebau, and F. Maglia, "Advances in battery technologies for electric vehicles," *Elsevier*, vol. 12, pp. 359-387, Jan. 2015.

[9] Y. Qiu and F. Jiang, "A review on passive and active strategies of enhancing the safety of lithium-ion batteries," *International Journal of Heat and Mass Transfer*, vol. 184, Dec. 2022.

[10] Y. Pan, Y. Zhu, and Y. Li *et al.*, "Homonuclear transition-metal dimers embedded monolayer C2N as promising anchoring and electrocatalytic materials for lithium-sulfur battery: first-principles calculations," *Applied Surface Science*, vol. 610, Feb. 2023.

[11] X. Zhang, Z. Li, and L. Luo *et al.*, "A review on thermal management of lithium-ion batteries for electric vehicles," *Energy*, vol. 238, Jan. 2022.

[12] P. Knauth, "Inorganic solid Li ion conductors: an over-

view," *Solid State Ionics*, vol. 180, no. 14-16, pp. 911-916, Jul. 2009.

[13] K. A. Smith, "Electrochemical control of lithium-ion batteries applications of control," *IEEE Control Systems Magazine*, vol. 30, no. 2, pp. 18-25, Feb. 2010.

[14] Y. Mekonnen, A. Sundararajan, and A. I. Sarwat, "A review of cathode and anode materials for lithium-ion batteries," in *SoutheastCon 2016*, pp. 1-6, Jul. 2016.

[15] X. Han, L. Lu, and Y. Zheng *et al.*, "A review on the key issues of the lithium ion battery degradation among the whole life cycle," *ETransportation*, vol. 1, Jan. 2019.

[16] O. Erdinc, B. Vural, and M. Uzunoglu, "A dynamic lithium-ion battery model considering the effects of temperature and capacity fading," in *2009 International Conference on Clean Electrical Power*, Capri, Italy, Jun. 2009.

[17] X. Hu, L. Xu, and X. Lin *et al.*, "Battery lifetime prognostics," *Joule*, vol. 4, no. 2, pp. 310-346, Feb. 2020.

[18] S. Cui, S. Riaz, and K. Wang, "Study on lifetime decline prediction of lithium-ion capacitors," *Energies*, vol. 16, no. 22, Nov. 2023.

[19] J. S. Edge, S. O'Kane, and R. Prosser *et al.*, "Lithium ion battery degradation: what you need to know," *Physical Chemistry Chemical Physics*, vol. 23, no. 14, pp. 8200-8221, Jul. 2021.

[20] J. Zhu, Y. Wang, and Y. Huang *et al.*, "Data-driven capacity estimation of commercial lithium-ion batteries from voltage relaxation," *Nature Communications*, vol. 13, no. 1, Jan. 2022.

[21] X. Tang, K. Liu, and K. Li *et al.*, "Recovering large-scale battery aging dataset with machine learning," *Patterns*, vol. 2, no. 8, Aug. 2021.

[22] P. K. Jones, U. Stimming, and A. A. Lee, "Impedance-based forecasting of lithium-ion battery performance amid uneven usage," *Nature Communications*, vol. 13, no. 1, Jan. 2022.

[23] Y. Zhang, Q. Tang, and Y. Zhang *et al.*, "Identifying degradation patterns of lithium ion batteries from impedance spectroscopy using machine learning," *Nature Communications*, vol. 11, no. 1, Jan. 2020.

[24] G. Ma, S. Xu, and B. Jiang *et al.*, "Real-time personalized health status prediction of lithium-ion batteries using deep transfer learning," *Energy & Environmental Science*, vol. 15, no. 10, pp. 4083-4094, Oct. 2022.

[25] G. Pozzato, A. Allam, and S. Onori, "Lithium-ion battery aging dataset based on electric vehicle real-driving profiles," *Data in Brief*, vol. 41, Feb. 2022.

[26] T. Raj, A. Wang, and C. Monroe *et al.*, "Investigation of path-dependent degradation in lithium-ion batteries," *Batteries Supercaps*, vol. 3, pp. 1377-1385, Aug. 2020.

[27] W. Li, H. Zhang, and B. van Vlijmen *et al.*, "Forecasting battery capacity and power degradation with multi-task learning," *Energy Storage Materials*, vol. 53, pp. 453-466, Sept. 2022.

[28] K. A. Severson, P. M. Attia, and N. Jin *et al.*, "Data-driven prediction of battery cycle life before capacity degradation," *Nature Energy*, vol. 4, no. 5, pp. 383-391, Sept. 2019.

[29] P. M. Attia, A. Grover, and N. Jin *et al.*, "Closed-loop optimization of fast-charging protocols for batteries with machine learning," *Nature*, vol. 578, no. 7795, pp. 397-402, Feb. 2020.

[30] Y. Che, X. Hu, and X. Lin *et al.*, "Health prognostics for lithium-ion batteries: mechanisms, methods, and prospects," *Energy & Environmental Science*, vol. 16, no. 2, pp. 338-371, Feb. 2023.

[31] J. Zhu, W. Xu, and M. Knapp *et al.*, "A method to prolong lithium-ion battery life during the full life cycle," *Cell Reports Physical Science*, vol. 4, no. 7, Jul. 2023.

[32] Z. Liu, C. Tan and F. Leng, "A reliability-based design concept for lithium-ion battery pack in electric vehicles," *Reliability Engineering & System Safety*, vol. 134, pp. 169-177, Oct. 2015.

[33] H. Shi, L. Wang, and S. Wang *et al.*, "A novel lumped thermal characteristic modeling strategy for the online adaptive temperature and parameter co-estimation of vehicle lithium-ion batteries," *Journal of Energy Storage*, vol. 50, Mar. 2022.

[34] H. Shi, S. Wang, J. Liang *et al.*, "Multi-time scale identification of key kinetic processes for lithium-ion batteries considering variable characteristic frequency," *Journal of Energy Chemistry*, vol. 82, pp. 521-536, Feb. 2023.

[35] K. Huang, Y. Wang, and J. Feng, "Research on equivalent circuit model of lithium-ion battery for electric vehicles," in *2020 3rd World Conference on Mechanical Engineering and Intelligent Manufacturing (WCMEIM)*, Shanghai, China, Dec. 2020.

[36] S. Saxena, S. R. Raman, and B. Saritha *et al.*, "A novel approach for electrical circuit modeling of Li-ion battery for predicting the steady-state and dynamic I–V characteristics," *Sādhanā*, vol. 41, pp. 479-487, May 2016.

[37] C. Zhang, J. Jiang, and W. Zhang *et al.*, "Estimation of state of charge of lithium-ion batteries used in HEV using robust extended Kalman filtering," *Energies*, vol. 5, no. 4, pp. 1098-1115, Apr. 2012.

[38] R. Xiong, J. Tian, and W. Shen *et al.*, "A novel fractional order model for state of charge estimation in lithium ion batteries," *IEEE Transactions on Vehicular Technology*, vol. 68, no. 5, pp. 4130-4139, May 2019.

[39] Y. Liu, L. Wang, and D. Li *et al.*, "State-of-health estimation of lithium-ion batteries based on electrochemical impedance spectroscopy: a review," *Protection and Control of Modern Power Systems*, vol. 8, no. 3, pp. 1-17, Jul. 2023.

[40] X. Sun, Y. Zhang, and Y. Zhang *et al.*, "Summary of health-state estimation of lithium-ion batteries based on electrochemical impedance spectroscopy," *Energies*, vol. 16, no. 15, Jul. 2023.

[41] Y. Liu, Q. Li, and K. Wang, "Revealing the degradation patterns of lithium-ion batteries from impedance spectroscopy using variational auto-encoders," *Energy Storage Materials*, vol. 69, Apr. 2024.

[42] Y. Li, B. Dong, and T. Zerrin *et al.*, "State-of-health

prediction for lithium-ion batteries via electrochemical impedance spectroscopy and artificial neural networks," *Energy Storage*, vol. 2, no. 5, Jun. 2020.

[43] R. Xiao, J. Shen, and X. Li *et al.*, "Comparisons of modeling and state of charge estimation for lithium-ion battery based on fractional order and integral order methods," *Energies*, vol. 9, no. 3, pp. 184, Mar. 2016.

[44] Y. Gao, K. Liu, and C. Zhu *et al.*, "Co-estimation of state-of-charge and state-of-health for lithium-ion batteries using an enhanced electrochemical model," *IEEE Transactions on Industrial Electronics*, vol. 69, no. 3, pp. 2684-2696, Mar. 2021.

[45] X. Zhang, Y. Gao, and B. Guo *et al.*, "A novel quantitative electrochemical aging model considering side reactions for lithium-ion batteries," *Electrochimica Acta*, vol. 343, Mar. 2020.

[46] C. Zhang, L. Luo, and Z. Yang *et al.*, "Battery SOH estimation method based on gradual decreasing current, double correlation analysis and GRU," *Green Energy and Intelligent Transportation*, vol. 2, no. 5, May 2023.

[47] N. A. Chaturvedi, R. Klein, and J. Christensen *et al.*, "Modeling, estimation, and control challenges for lithium-ion batteries," in *Proceedings of the 2010 American Control Conference*, Baltimore, MD, USA, Jun. 2010.

[48] G. Zhu, C. Kong, and J. V. Wang *et al.*, "A fractional-order electrochemical lithium-ion batteries model considering electrolyte polarization and aging mechanism for state of health estimation," *Journal of Energy Storage*, vol. 72, Aug. 2023.

[49] M. Hossain, M. Haque and M. T. Arif, "Kalman filtering techniques for the online model parameters and state of charge estimation of the Li-ion batteries: a comparative analysis," *Journal of Energy Storage*, vol. 51, Mar. 2022.

[50] X. Sun, K. Zhong, and M. Han, "A hybrid prognostic strategy with unscented particle filter and optimized multiple kernel relevance vector machine for lithium-ion battery," *Measurement*, vol. 170, Nov. 2021.

[51] I. O. Santos-Mendoza, E. R. Henquín, and J. Vazquez-Arenas *et al.*, "Simplified electrochemical model to account for different active/inactive cathode compositions in Li-ion batteries," *Journal of Energy Storage*, vol. 31, Jun. 2020.

[52] D. Liu, X. Yin, and Y. Song *et al.*, "An on-line state of health estimation of lithium-ion battery using unscented particle filter," *IEEE Access*, vol. 6, pp. 40990-41001, Dec. 2018.

[53] Y. Ma, M. Yao, and H. Liu *et al.*, "State of health estimation and remaining useful life prediction for lithium-ion batteries by improved particle swarm optimization-back propagation neural network," *Journal of Energy Storage*, vol. 52, May 2022.

[54] M. Ahwiadi and W. Wang, "An enhanced particle filter technology for battery system state estimation and RUL prediction," *Measurement*, vol. 191, Feb. 2022.

[55] Y. Zhang and Y. Li, "Prognostics and health management of Lithium-ion battery using deep learning methods: a review," *Renewable and Sustainable Energy Reviews*, vol. 161, Mar. 2022.

[56] Z. Chen, M. Sun, and X. Shu *et al.*, "On-board state of health estimation for lithium-ion batteries based on random forest," in *2018 IEEE International Conference on Industrial Technology (ICIT)*, Lyon, France, Feb. 2018.

[57] Y. Li, C. Zou, and M. Berecibar *et al.*, "Random forest regression for online capacity estimation of lithium-ion batteries," *Applied Energy*, vol. 232, pp. 197-210, Oct. 2018.

[58] H. Xiang, Y. Xi, and D. Mao *et al.*, "Mapping potential wetlands by a new framework method using random forest algorithm and big Earth data: a case study in China's Yangtze River Basin," *Global Ecology and Conservation*, vol. 42, Feb. 2023.

[59] Y. Li, E. Herrera-Viedma, and G. Kou *et al.*, "Z-number-valued rule-based decision trees," *Information Sciences*, vol. 643, May 2023.

[60] H. Hao, F. Fuzhou, and Z. Junzhen *et al.*, "Research on fault diagnosis method based on improved CNN," *Shock and Vibration*, vol. 2022, 2022.

[61] B. Li, R. Li, and T. Sun *et al.*, "Improving LSTM hydrological modeling with spatiotemporal deep learning and multi-task learning: a case study of three mountainous areas on the Tibetan Plateau," *Journal of Hydrology*, vol. 620, 2023.

[62] S. M. Moghadam, T. Yeung, and J. Choisne, "A comparison of machine learning models' accuracy in predicting lower-limb joints' kinematics, kinetics, and muscle forces from wearable sensors," *Scientific Reports*, vol. 13, no. 1, Jan. 2023.

[63] A. M. N. Ribeiro, P. R. X. do Carmo, and P. T. Endo *et al.*, "Short-and very short-term firm-level load forecasting for warehouses: a comparison of machine learning and deep learning models," *Energies*, vol. 15, no. 3, Mar. 2022.

[64] C. Qiu, Q. Wang, and F. Xie *et al.*, "Prediction method of full-condition and high-precision current of asynchronous motors for electric vehicles based on XGBoost," *Proceedings of the CSEE*, vol. 40, pp. 313-322, 2020. (in Chinese)

[65] S. Wu, Q. Yuan, and Z. Yan *et al.*, "Analyzing accident injury severity via an extreme gradient boosting (XGBoost) model," *Journal of Advanced Transportation*, vol. 2021, pp. 1-11, 2021.

[66] A. Ogunleye and Q. Wang, "XGBoost model for chronic kidney disease diagnosis," IEEE/ACM Transactions on Computational Biology and Bioinformatics, vol. 17, no. 6, pp. 2131-2140, Nov. 2020.

[67] G. Lee, D. Kwon, and C. Lee, "A convolutional neural network model for SOH estimation of Li-ion batteries with physical interpretability," *Mechanical Systems and Signal Processing*, vol. 188, Dec. 2023.

[68] S. Ji, J. Zhu, Z. Lü *et al.*, "Deep learning enhanced lithium-ion battery nonlinear fading prognosis," *Journal of Energy Chemistry*, vol. 78, pp. 565-573, Jan. 2023.

[69] W. S. McCulloch and W. Pitts, "A logical calculus of the ideas immanent in nervous activity," *The Bulletin of Mathematical Biophysics*, vol. 5, pp. 115-133, 1943.

[70] J. Gao, D. Yang, and S. Wang *et al.*, "State of health estimation of lithium-ion batteries based on mixers-bidirectional temporal convolutional neural network," *Journal of Energy Storage*, vol. 73, Oct. 2023.

[71] L. Zhang, K. Wang, and B. Zhong, "Battery health state prediction based on lightweight neural networks: a review," *Ionics*, vol. 30, no. 12, pp. 7781-7807, Oct. 2024.

[72] X. Yu, T. Ai, and K. Wang, "Application of nanogenerators in acoustics based on artificial intelligence and machine learning," *APL Materials*, vol. 12, no. 2, Feb. 2024.

[73] J. Meng, M. Yue, and D. Diallo, "A degradation empirical-model-free battery end-of-life prediction framework based on Gaussian process regression and Kalman filter," *IEEE Transactions on Transportation Electrification*, vol. 9, no. 4, pp. 4898-4908, Dec. 2023.

[74] B. Duan, Q. Zhang, and F. Geng *et al.*, "Remaining useful life prediction of lithium-ion battery based on extended Kalman particle filter," *International Journal of Energy Research*, vol. 44, no. 3, pp. 1724-1734, Mar. 2020.

[75] H. Ruan, J. Chen, and W. Ai *et al.*, "Generalised diagnostic framework for rapid battery degradation quantification with deep learning," *Energy and AI*, vol. 9, Sept. 2022.

[76] A. Saxe, S. Nelli, and C. Summerfield, "If deep learning is the answer, what is the question?," *Nature Reviews Neuroscience*, vol. 22, no. 1, pp. 55-67, Nov. 2020.

[77] A. Farmann, W. Wang, and A. Marongiu *et al.*, "Critical review of on-board capacity estimation techniques for lithium-ion batteries in electric and hybrid electric vehicles," *Journal of Power Sources*, vol. 281, pp. 114-130, Jan. 2015.

[78] H. Knobloch, A. Frenk, and W. Chang, "Predicting battery lifetime with CNNs," *Towards Data Science, https://towardsdatascience.com/predicting-battery-lifetime-with-cnns-c5e1faeecc8f*, 2019.

[79] Y. Zheng, Y. Che, and X. Hu *et al.*, "Thermal state monitoring of lithium-ion batteries: progress, challenges, and opportunities," *Progress in Energy and Combustion Science*, vol. 100, Sept. 2024.

[80] Y. Che, Y. Zheng, and X. Sui *et al.*, "Boosting battery state of health estimation based on self-supervised learning," *Journal of Energy Chemistry*, vol. 84, pp. 335-346, Jul. 2023.

[81] G. Qi, N. Ma, and K. Wang, "Predicting the remaining useful life of supercapacitors under different operating conditions," *Energies*, vol. 17, no. 11, May 2024.

[82] P. Burlina, "MRCNN: a stateful fast R-CNN," in *2016 23rd International Conference on Pattern Recognition (ICPR)*, Cancun, Mexico, Dec. 2016.

[83] Y. Che, F. Forest, and Y. Zheng *et al.*, "Health prediction for lithium-ion batteries under unseen working conditions," *IEEE Transactions on Industrial Electronics*, vol. 71, no. 11, pp. 14254-14264, Nov. 2024.